Int. J. Radiat. Biol., 2010, Early Online, pp. 1–17

informa
healthcare

Proteomic and genomic modulations induced by γ-irradiation of human blood lymphocytes

ANDREI TURTOI[1], RAJESHWAR N. SHARAN[2], ALOK SRIVASTAVA[3] & FRANK H. A. SCHNEEWEISS[1]

[1]*Laboratory of Radiation Biology, Department of Safety and Radiation Protection, Research Centre Jülich, Jülich, Germany,* [2]*Department of Biochemistry, North-Eastern Hill University, Shillong, Meghalaya, and* [3]*Chemistry Department, Panjab University, Chandigarh, India*

(Received 26 January 2009; Revised 8 April 2010; Accepted 9 April 2010)

Abstract

Purpose: Quantitative evaluation of early response proteins (ERPRO) and early response genes (ERG) following γ-irradiation of human lymphocytes; identification of specific proteins and genes as candidate biomarkers for the development of a novel biodosimeter.

Materials and methods: Human peripheral blood lymphocytes were exposed to clinically relevant doses (1, 2 and 4 Gy) of γ-radiation ex-vivo. Analyses of protein and gene expression modulation were conducted 2 h post-irradiation. Global modulations were monitored using two-dimensional polyacrylamide gel electrophoresis (2D-PAGE) and DNA microarray analyses of the samples originating from one human donor. On the proteome level, both phosphorylated and non-phosphorylated proteins were considered. Proteins and genes of specific interest were further targeted using Western blot (WB) and real-time quantitative polymerase chain reaction (RT-qPCR) techniques, employing samples from several human donors ($n = 3$).

Results: A set of ERPRO and ERG showing significant alterations 2 h post-γ-irradiation have been identified in human lymphocytes. The most radiation responsive genes and proteins indicated alterations of cellular structure (β-actin, talin-1 [TLN1], talin-2, zyxin-2), immune and defence reactions (major histocompatibility complex binding protein-2 [MBP2], interleukin-17E and interferon-γ), cell cycle control (cyclin-dependent kinase inhibitor-1A [CDKN1A], mouse double minute-2, annexin-A6 [ANXA6], growth arrest and DNA-damage-inducible protein-α [GADD45A], proliferating cell nuclear antigen [PCNA], dual specificity phosphatase-2 and 8 [DUSP8]) as well as detoxification processes (peroxin-1) and apoptosis (B-cell lymphoma-2 binding component-3 [BBC3]).

Summary: The estimations of protein concentration modulation of TLN1 and CDKN1A, phosphorylation status of ANXA6 (dose range 0–2 Gy) and MBP2 as well as the alterations in the level of gene expressions of BBC3, DUSP8, GADD45A and PCNA appears to be of potential value for future biodosimetric applications.

Keywords: *genomic analysis, proteomics, γ-radiation, human blood lymphocytes, biodosimeter*

Introduction

A study of radiation-induced early alterations in mammalian cells can play an important role in the understanding cell differentiation, malignant transformation and cell death. The progress in the fields of proteomics using two-dimensional polyacrylamide gel electrophoresis (2D-PAGE), mass spectrometry (MS) and genomics using DNA microarrays has opened up new possibilities to understand these early events. The identification of early response proteins (ERPRO) and early response genes (ERG) can potentially give deeper insights into the radiation-induced cellular injuries, which are of particular interest both in radiation therapy and protection programs. Several studies addressing these issues have produced a pool of potential protein biomarkers of γ-exposure. In one such study, Szkanderova et al. (2003) identified 10 proteins in murine fibroblasts 20 min to 72 h after 240 kVp X-ray irradiation (6 Gy). All of these proteins were related to metabolism and involved with cell proliferation, glycolysis or protein folding and degradation. However, no significant correlation was reported between

Correspondence: Dr Andrei Turtoi, Mass Spectrometry Laboratory, Department of Chemistry, University of Liege, Bat. B6c, B-4000 Liege, Belgium. Fax: +32 4 3663413. E-mail: a.turtoi@ulg.ac.be

ISSN 0955-3002 print/ISSN 1362-3095 online © 2010 Informa UK Ltd.
DOI: 10.3109/09553002.2010.486016

the changes observed at the level of protein concentration and the expression of corresponding genes suggesting difficulty of using the gene expression data to deduce the reciprocal protein perturbation. In another study employing 2D-PAGE and MS analyses, Szkanderova et al. (2005) showed a time-dependent (2.5 and 12 h post-irradiation) response of 14 proteins in human T-lymphocyte leukemia cells after their exposure to 7.5 Gy of ^{60}Co γ-rays. These proteins were also metabolically important and associated with various cell signalling pathways, and protein degradation, malignant transformation and detoxification processes. Marchetti et al. (2006) summarised the results of radiation-induced protein alterations ranking the identified proteins on their potential suitability for biodosimetric applications. Turtoi et al. (2007) further identified five ERPRO in human blood lymphocytes 15 min after exposure to ^{137}Cs γ-rays (2 Gy) that were associated with the cytoskeleton and cellular glycolysis. These studies clearly indicate that ERPRO could indeed be used as biodosimetric markers of exposure to γ-rays. Recently Ossetrova et al. (2007) showed that the protein concentrations of cyclin-dependent kinase inhibitor-1A (CDKN1A), interleukin-6, salivary amylase and c-reactive protein in blood serum of non-human primates could be reliable dose indicators after whole body exposure to 250 kVp X-rays (6 Gy) in vivo. These encouraging results point at the possibility that similar measurements could be possible in humans as well. However, the development of precise, biomarker-based, dosimetric applications precludes the discovery of genes or proteins, which are specific to ionising radiation and would respond to medical relevant levels of radiation exposure. Some of the above proteins, namely c-reactive protein and interleukin-6, are known to be elevated in acute phase inflammatory reactions (Whiteley et al. 2009) and not only in response to ionising radiation. Therefore, their elevated levels may give rise to false positives. Likewise, alterations of markers like the CDKN1A are often encountered in cases of radiation and cytotoxic insults (e.g., non-ionising ultra-violet [UV] radiations, free radicals, etc.) (Fotedar et al. 2004) and cannot alone confer the required specificity to a potential biodosimeter. Along these lines, current endeavours are directed towards the discovery of specific and radiation responsive markers which would make such biodosimetric applications feasible.

Along the identification of radiation-responsive proteins, DNA microarray-based gene expression studies have also attempted to find suitable candidate ERG to serve as biomarkers of radiation exposure. A series of genome-wide screening of various cell types have been performed raising the pool of potential markers for human exposure to γ-radiations (Amundson et al. 2000, 2004, Kang et al. 2003, Dressman et al. 2007). Using the DNA microarray approach, we have identified 102 ERG in human peripheral blood lymphocytes exposed to γ-radiation (Turtoi et al. 2008). Fourteen of the ERG have been validated by real-time quantitative polymerase chain reaction (RT-qPCR) in six individuals. Five of these genes appear to be potentially suitable as biodosimetric markers, e.g., early growth response protein-1 (EGR1), early growth response protein-4 (EGR4), interferon-γ (IFN-γ), cytoplasmic jun oncogene (c-JUN) and tumour necrosis factor superfamily member-9 (TNFSF9).

Although the measurement of radiation dose-dependent alteration of protein concentrations has ultimate biological relevance, the global proteomic analysis alone may not provide a complete picture of the radiation-induced cellular changes. The most important reason for this is the inability of such analyses to cover large dynamic ranges of protein concentrations (currently up to maximum 3–4 orders of magnitude). Genomic analyses by DNA microarrays are more sensitive (approximately 7 orders of magnitude). But, again, the modulated gene expression alone does not necessarily correlate with the actual cellular response. The likely solution to this problem would be monitoring the modulations of both gene expression and protein concentration. Until now, there is a dearth of studies that simultaneously assess the radiation-induced biological modifications at transcriptional, translational and post-translational levels. The present study was designed to fill this void wherein proteomic and genomic analyses have been combined to obtain a more holistic picture of cellular response. The objective was to come up with a series of radiation-sensitive early response proteins and genes that are altered in human lymphocytes exposed to γ-irradiation in a medically relevant dose range. As a consequence, several differentially modulated proteins have been identified. Of these, a selected group was further investigated for corresponding gene expression modulations using RT-qPCR. Simultaneously, another screening was conducted on the gene expression level using the whole human genome DNA microarrays. More than 40 differentially expressed genes have been identified. Four of them were selected four were selected and their corresponding protein modulations were analysed by WB. Finally, five ERG and four ERPRO were validated for their differential modulations following ex-vivo γ-irradiation of human blood lymphocytes obtained from three individual donors. This two-way approach – one starting from the protein level and the other from the gene expression stage – should provide a more complete picture of the early alterations taking place in human blood lymphocytes

exposed to increasing dose of γ-radiation in a clinically relevant dose range (see Figure 1).

Materials and methods

Unless otherwise indicated, all chemicals (highest quality available) were purchased from Sigma-Aldrich Co. (St Louis, MO, USA). Both global proteomic (2D-PAGE) and genomic (DNA microarrays) analyses were conducted using samples originating from one human donor (individual 1, male, 30 years). Modulated genes and proteins identified from these investigations were further validated using RT-qPCR and WB in two additional human donors (individual 2, male, 29 years, and individual 3, female, 31 years). All three informed and consenting human volunteers were healthy, non-smokers and took no medication during the period of investigation. The purpose of this project and the experiments undertaken complied with the regulations and ethical guidelines of the Research Centre Juelich, Germany.

Irradiation, isolation of blood lymphocytes, and preparation of protein and RNA extracts

Heparinised blood drawn from the donor (each donor was sampled three times on three consecutive days) was irradiated with ^{137}Cs γ-rays (Gammacell 40, Atomic Energy Canada, Mississauga, ON, Canada). Whole blood specimens (6 ml) received radiation doses of 1.0, 2.0 and 4.0 Gy delivered at a dose rate of 0.8 Gy/min at 37°C. Immediately after irradiation, lymphocytes were isolated by density-gradient centrifugation using Ficoll-Paque PLUS (GE Healthcare, Piscataway, NJ, USA). One part of the isolated lymphocytes (3×10^6 cells) was lysed in 1 ml ice cold lysis buffer (30 mM tris-HCl, 2 M thiourea, 7 M urea, 4% 3-[(3-Cholamidopropyl)-dimethylammonio]- 1-propanesulfonate (CHAPS), protease and phosphatase inhibitor cocktail (Roche, Mannheim, Germany), pH 8.0) followed by the protein extraction and precipitation using the 2D Clean-Up Kit (GE Healthcare).

The second aliquot of the lymphocytes was used for RNA isolation. For this purpose, approximately 3×10^6 lymphocytes were transferred into 1 ml Trizol® (Invitrogen, Carlsbad, CA, USA) reagent, vortexed and centrifuged at 12,000 *g* for 10 min. The supernatant was mixed with 200 μl chloroform and centrifuged. Clear RNA containing upper phase was recovered. The RNA was precipitated using 500 μl isopropanol and was washed with 2 ml of 75% ethanol. After a brief desiccation at room temperature, the RNA pellet was dissolved in 50 μl of RNase-free water. The quantification and control of the integrity of the RNA was performed using Bioanalyzer 2100 (Agilent Technologies, Santa Clara, CA, USA). All samples used had a RNA integrity number (RIN, Agilent) ranging from 8–10 indicating the highest quality RNA specimen.

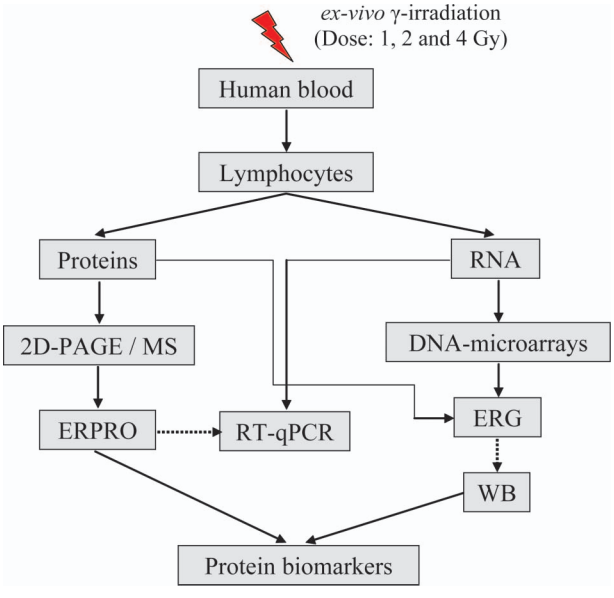

Figure 1. The flow chart gives an overview of the experimental protocol followed in this investigation. The interrupted arrow pointing from ERPRO towards RT-qPCR indicates that the information obtained from the ERPRO was used to select the genes whose expressions were studied using the RT-qPCR. Similarly, the interrupted arrow pointing from ERG towards WB indicates that the information from ERG was used to select the proteins to be analysed with WB.

Protein analysis by 2D-PAGE

The protein sample from individual 1 (130 μg) was dissolved in 300 μl of rehydratation buffer (7 M urea, 2% CHAPS, 0.5% ampholytes pH 3–10 (Invitrogen), 0.05% bromophenol blue and 20 mM 1,4-dithio-DL-threitol [DTT]) and incubated overnight with the immobilised pH gradient (IPG) strips (17 cm, pH 3–10; BioRad, Hercules, CA, USA). Subsequently, the strips containing proteins were subjected to isoelectric focussing (IEF) at 20°C in a PROTEAN-IEF Cell (BioRad). The IEF run was for 20 min at 250 V followed by 2.5 h at 250–10,000 V linear gradient or until 40,000 Vh had accumulated. Following the IEF run, the IPG strips were incubated for 10 min in buffer 1 (50 mM DTT in 5 ml 1X NuPage lithium dodecyl sulfate [LDS] Sample Buffer™ (Invitrogen) followed by 10 min in buffer 2 (125 mM iodoacetamide in 5 ml 1X NuPage LDS Sample-Buffer™).

The second dimension sodium dodecyl sulphate-polyacrylamide gel electrophoresis (SDS-PAGE) was conducted using PROTEAN-II (19°C, 16 mA/gel for 30 min, followed by 24 mA/gel

for ~5 h) employing 12% gels (40 ml 30% acrylamide/bis-acrylamide, 25 ml 1.5 M tris-HCl (pH 8.8), 1 ml 10% SDS, 500 μl 10% ammoniumpersulfate, 50 μl tetramethylethylenediamine (TEMED); final volume made up to 100 ml with water) and tris-glycine buffer (6.6 g tris-base, 28.8 g glycine and 2.0 g SDS in 2.0 l water). The gels were stained and visualised using: (i) The phosphoprotein fluorescence dye Pro-Q Diamond (535 nm green laser with 575 nm low-pass [LP] filter) as well as (ii) total protein dye Sypro Ruby (473 nm blue laser with 530 nm dual-pass [DP] 20 filter). Both dyes were obtained from Invitrogen. The specific phosphoprotein fluorescent dye reacts with the phosphate groups attached to tyrosine, serine or threonine residues. The respective signal intensity is linear over three orders of magnitude and correlates with the number of phosphate groups. The colouration does not allow distinguishing between the increase of the protein amount or its phosphorylation status. In the present study, a phosphoprotein is considered changed in its phosphorylation status if not found altered in the total proteome analysis. Otherwise and in the case of the total protein study, the spot volumes are considered equivalent to the protein concentrations for all the proteins which were uniquely identified in the MS analysis within the corresponding 2D spot.

The 2D-PAGE gel was analysed using the FLA5000 laser scanner (Fuji Film, Tokyo, Japan) at 100 μm resolution. The images and the corresponding optical densities were analysed with the Delta 2D software 3.3 (Decodon, Greifswald, Germany). Only spots showing significant changes of intensity (two-sided, unpaired Student's *t*-test, assuming equal variances with an error probability of $P \leq 0.05$, $n = 3$) and greater than two-fold increase or decrease in magnitude of relative concentration for both 2 and 4 Gy samples were selected for further analysis (exact statistics are provided in supplemental data Table I, available online).

Table I. TaqMan™ assays used for the RT-qPCR gene expression measurements of selected ERPRO and ERG. The manufacturing ID codes correspond to the assays provided by Applied Biosystems (see www.appliedbiosystems.com).

Gene Symbol	Manuf. ID
ANXA6	Hs00241765_m1
ACTB	Hs99999903_m1
BBC3	Hs00248075_m1
DUSP8	Hs01014943_m1
GADD45A	Hs00169255_m1
LAP1B	Hs00397345_m1
PCNA	Hs00427214_g1
PGK1	Hs99999906_m1
TLN2	Hs00322257_m1
TRAF4	Hs00188755_m1

MS analysis and protein identification

The gel spots of interest were excised from a preparative gel (12% SDS-PAGE with 300 μg protein load) using Proteineer SP II spot-picking robot (Bruker, Bremen, Germany). They were transferred to a 96-well plate and further processed using the Janus pipetting robot (Perkin Elmer, Waltham, MA, USA). The gel spots were rinsed in 50 mM bicarbonate buffer, destained with acetonitrile and digested using trypsin (Promega, Madison, WI, USA) overnight (16 h) at 37°C. The peptides were extracted in ultra-pure water containing 20% acetonitrile and 0.5% formic acid. Following desiccation and solubilisation in 20 μl water and 0.1% formic acid, the peptide containing samples were analysed using the 1D-nano-high performance liquid chromatography (HPLC) (Eksigent, Dublin, CA, USA) coupled with the ESI-QTrap-2000 MS (Applied Biosystems, Foster City, CA, USA). After the sample injection in the HPLC system, the peptides were desalted online using the C18 pre-column (Acclaim PepMap, 300 μm i.d. × 5 mm; Dionex, Sunnyvale, CA, USA) for 5 min at a flow rate of 20 μl/min (97.9% water, 2% acetonitrile and 0.1% formic acid). The separation of the peptides was performed using the analytical C18 column (Acclaim 75 μm × 150 mm; Dionex) and a 45 min solvent gradient (t = 0 min, 0% B [B: 97.9% acetonitrile, 2% water and 0.1% formic acid]; t = 45 min, 40% B) at the flow rate of 0.3 μl/min. The MS scanned the mass range from 400–1200 m/z (linear ion trap fill time was set to dynamic mode). The three most intense peptides found in this mass range, barring + 2 and + 3 charges, were preferentially and automatically fragmented in MS/MS mode (m/z range: 100–2000, rolling collision energy default settings, linear ion trap fill time set at 250 ms). Protein identification was conducted using the Mascot Search Engine Version 2.1 (Matrix Sciences, Boston, MA, USA) and the human non-redundant and non-identical protein database Swiss-Prot (Swiss Institute of Bioinformatics, Basel, Switzerland, release 57.0; 20,334 entries). Following parameters were used: MS tolerance 0.6 Da, MS/MS tolerance 0.3 Da, 1 missed cleavage was allowed, carbamidomethylation was set as fixed whereas oxidation and phosphorylation were variable modifications.

Quantitative gene expression study by DNA-microarray

The global gene expression analysis was performed using the whole human genome 4 × 44K DNA microarrays (Agilent Technologies). Three replicates originating from one human individual were used for each dose. The isolated total RNA (0.4 μg) was converted into Cy3-cRNA using the Low RNA Input

Linear Amplification Kit (Agilent Technologies). The labelled cRNA was then purified using the RNeasy Kit (Qiagen, Hilden, Germany). The purified Cy3-labelled cRNA (1.65 μg) was fragmented and hybridised under rotation (10 rpm) at 65°C for 17 h on the 4 × 44K array using the Gene Expression Hybridization Kit (Agilent Technologies). The arrays were washed in GE wash buffer-1 and 2 followed by immediate analysis. The data were accrued on the Agilent Microarray Scanner and processed with the GeneSpring 7 software to generate ratios of relative gene expression (RE) of the irradiated vs. non-irradiated samples. For statistical evaluation, a one-way ANOVA test (parametric, unequal variances, including Benjamini-Hochberg false discovery rate multiple testing correction combined with Tukey post-hoc test at the false positive rate $P \leq 0.05$, $n = 3$) was employed for the initial screening. Only those genes showing a significant ($P \leq 0.05$), minimum two-fold up- or down-regulation in at least one of the irradiated samples with respect to the controls were considered for the final evaluation (see Table II).

Quantitative analysis of gene expression by RT-qPCR

Gene expressions of four proteins, namely annexin-6 (ANXA6), talin-2 (TLN2), β-actin (ACTB) and phosphoglycerate kinase-1 (PGK1), which exhibited sustained dose response in at least three out of four dose points, were quantified by RT-qPCR using the TaqMan chemistry. In addition, the following five genes were validated for all three individual donors: B-cell lymphoma-2 binding component-3 (BBC3), dual specificity phosphatise-8 (DUSP8), growth arrest and DNA-damage-inducible protein-α (GADD45A), proliferating cell nuclear antigen (PCNA) and tumour necrosis factor receptor associated factor-4 (TRAF4). For this purpose, 1 μg of RNA was converted to cDNA using High-Capacity DNA-Archive Kit. The cDNA (10 ng) was dissolved in TaqMan PCR Mastermix containing the specific TaqMan probes. Standard PCR program (95°C for 15 s followed by 60°C for 1 min, applied for 50 cycles) was applied. The data evaluation was conducted using the Sequence Detection Software 1.3.1 (Applied Biosystems). The 18S-rRNA (Hs99999901_s1) TaqMan assay served as the endogenous control. For statistical evaluation, Excel software (Microsoft, Redmond, WA, USA) and the Student's *t*-test (two-sided, unpaired, assuming equal variances and an error probability of $P \leq 0.05$, $n = 3$) were used. The TaqMan assays were selected such that for a given gene the largest possible number of known splice forms could be detected. The assay ID of the corresponding TaqMan probes is shown in Table I.

WB analysis of selected proteins

Genes which showed altered level of expression following DNA microarray analysis were checked for alterations in their protein levels using WB. Four proteins namely, CDKN1A, PCNA, c-JUN and mouse double minute-2 (MDM2) were chosen for this analysis. The modulation of these proteins following γ-irradiation was monitored in three human individual donors.

Lymphocyte protein extract (25 μg) was dissolved in 15 μl sample buffer (8 M urea, 4% SDS, 100 mM DTT, 25% glycerol and 0.05% bromophenol blue) and loaded onto a 12% Novex bis-tris gel (Invitrogen) for electrophoresis (200 V and 20°C for 1 h) in 3-(N-morpholino) propanesulfonic acid (MOPS) buffer (10.46 g MOPS, 6.06 g tris-base, 1.0 g SDS and 0.3 g ethylenediamine tetraacetic acid in 1 l

Table II. Selected proteins from Figures 3 and 4 that displayed PEST sequence: Those proteins which had PEST sequence near the C terminus are marked with one asterisk (*) whereas those marked with two asterisk (**) had the sequence near the N terminus. The scores represent the potential biological relevance for protein degradation; higher scores mean greater relevance. The scores were calculated with EMBnet AUSTRIA software. For details, see: https://emb1.bcc.univie.ac.at/toolbox/pestfind/pestfind-analysis-webtool.htm.

Protein	PEST-sequence	**Score**
Talin-1	419 HFGLEGDEESTMLEDSVSPK 438	+5.80
Talin-2	422 RFGLEGDEESTMLEESVSPK 441	+6.12
Peroxine-1	1100 HSSGSDDSAGDGECGLDQSLVSLEMSEILPDESK 1133	+7.16*
MBP2	773 RPQLQPGSPSLVSEESPSAIDSDK 796	+8.15
	840 KAPSPSETCDSEISEAPVSPEWAPPGDGAESGGK 873	+13.68
	1516 KDGLQSGSSSFSSLSPSSSQDYPSVSPSSR 1545	+8.44
	1574 KESSDELDIDETASDMSMSPQSSSLPAGDGQLEEEGK 1610	+13.82
	1906 HQFSDAEESDGEDGDDNDDDDEDEDDFDDQGDLTPK 1941	+24.38
	2026 RLDIPSCMDEECMLPSEPSSSPR 2048	+6.55
Zyxin-2	51 RPGDSEPPPAPGAQR 65	+8.02**
	70 RVGEIPPPPPEDFPLPPPPLAGDGDDAEGALGGAFPPP PPPIEESFPPAPLEEEIFPSPPPPPEEEGGPEAPIPPPPQPR 149	+16.08**

water) using the X-Cell Sure Lock (Invitrogen) electrophoresis device. Subsequently, the resolved proteins on the gels were blotted onto 0.25 μm nitrocellulose membranes (Invitrogen) at 30 V. After 30 min, the lower part of the membrane containing the 10–30 kDa protein fractions was removed. The remaining protein fractions (40–60 kDa and 60–110 kDa) were blotted for additional 15 and 30 min, respectively. The target proteins were identified using the Qdot Kit (Invitrogen) as described below. After blotting, the membranes were washed in wash-buffer A, blocked with the blocking buffer at room temperature for 1 h, and incubated with corresponding primary antibodies in the same buffer overnight at 4°C under mild rocking. The concentrations of antibodies used for different proteins were: 1:500 dilution of rabbit anti-PCNA [ab-5] (Calbiochem, Nottingham, UK), 6 μg/ml rabbit anti c-JUN/AP1 [ab-2] (Calbiochem), 8 μg/ml CDKN1A (mouse anti $p21_{WAF1/CIP1}$; Sigma) and 4 μg/ml mouse anti-MDM2 (Sigma). All except c-JUN were monoclonal antibodies. After an overnight incubation, the membranes were washed in wash buffer A and incubated with Qdot secondary antibody (Qdot 655 goat anti-rabbit IgG and Qdot 565 goat anti-mouse IgG) conjugates (dilution 1:1000) in blocking buffer at room temperature for 2 h. The membranes were again washed in wash buffer A followed by wash buffer B prior to their imaging using the FLA5000 scanner (473 nm blue laser in combination with Cy3- and Cy5-emission filter for the Qdot 565 and 655 antibody, respectively) at a scan resolution of 100 μm. The image analysis was conducted with the help of the Aida Image Analyzer software platform 3.5 (Raytest, Straubenhardt, Germany). The normalisation was conducted using the alpha tubulin protein concentration (detected with mouse anti-alpha tubulin; cat. no. ab80779 [Abcam, Cambridge, MA, USA]). Proteins MDM2 and c-JUN normally display several variants and/or additional post-translational modifications. In this study for both proteins and within the corresponding molecular weight range, several bands were observed. All the visible bands were taken into consideration for the densitometric evaluation.

Results

MS-based identification of ERPRO

The 2D-PAGE analysis indicated at more than 20 proteins whose concentrations were altered following the exposure of lymphocytes to γ-radiation (disclosed in the proceedings of the ACREBS 2006 conference in Kolkata, India, and published as work in progress by Turtoi et al. 2007). These proteins were subjected to a detailed and individual MS identification, which included liquid chromatography and data-dependent MS analysis. The results obtained were compared with the amino acid sequences from the Swiss-Prot databank in order to identify corresponding proteins. A representative result of one of these 20 proteins, PGK1, is shown in Figure 2.

Among the modulated proteins, MS identified 11 radiosensitive candidate ERPRO (Figure 3). Five of these 11 ERPRO exhibited significant ($0.5 \geq \mathrm{RE} \geq 2.0$ and $P \leq 0.05$, in at least two out of three irradiated samples) down-regulation (Figure 4). Of these five ERPRO, four (TLN1 and 2, ACTB and mutant ACTB [mACTB]) are essentially structural proteins while the fifth, Peroxin-1 (PEX1), is involved in protein transport and degradation. The remaining 6 ERPRO (MBP2, PGK1, ANXA6, zyxin-2 (ZYX2), interleukin-17E (IL17E) and phosphorylated ACTB) exhibited significant up-regulation (Figure 5). Four of these proteins (MBP2, PGK1, ANXA6, and IL17E) are associated with the cell cycle control and immune system.

All the proteins that displayed significant modulations were further analysed for the presence of special amino acid sequences motif PEST (proline, glutamic acid, serine and threonine) that can determine their natural half-lives. Some specialised proteins like MDM2 exhibit ubiquitin ligase function and tag such motif containing proteins for proteosome degradation. Using EMBnet web tool, PEST-containing proteins have been scored indicating the biological relevance of each PEST sequence found. The algorithm screens hydrophilic regions of 12 and more amino acids containing at least one proline, glutamic acid, serine and threonine, flanked by lysine, arginine or histidine. The scores range from -50 to $+50$; values greater than $+5$ indicate significant PEST motifs with respect to the abundance of these motives in the entire genome. The results are shown in Table II. Of the proteins investigated, TLN1 and 2 as well as PEX1 appear to have at least one PEST motif each. The proteins MBP2 and ZYX2 have six and three PEST motifs, respectively. Since no specific measurements of the ubiquitination or oxidative damage were conducted, the results indicate a cumulative effect of these processes and ionising radiation. Nevertheless, the presence of such motifs may indicate that degradation processes are potentially responsible for the diminishing protein quantities following γ-irradiation.

Analysis of gene expression of selected ERPRO by RT-qPCR

The results of the relative expression analysis of four selected genes (ANXA6, ACTB, TLN2 and PGK1) using RT-qPCR are shown in Figure 6. These genes exhibited sustained dose responses. Since three

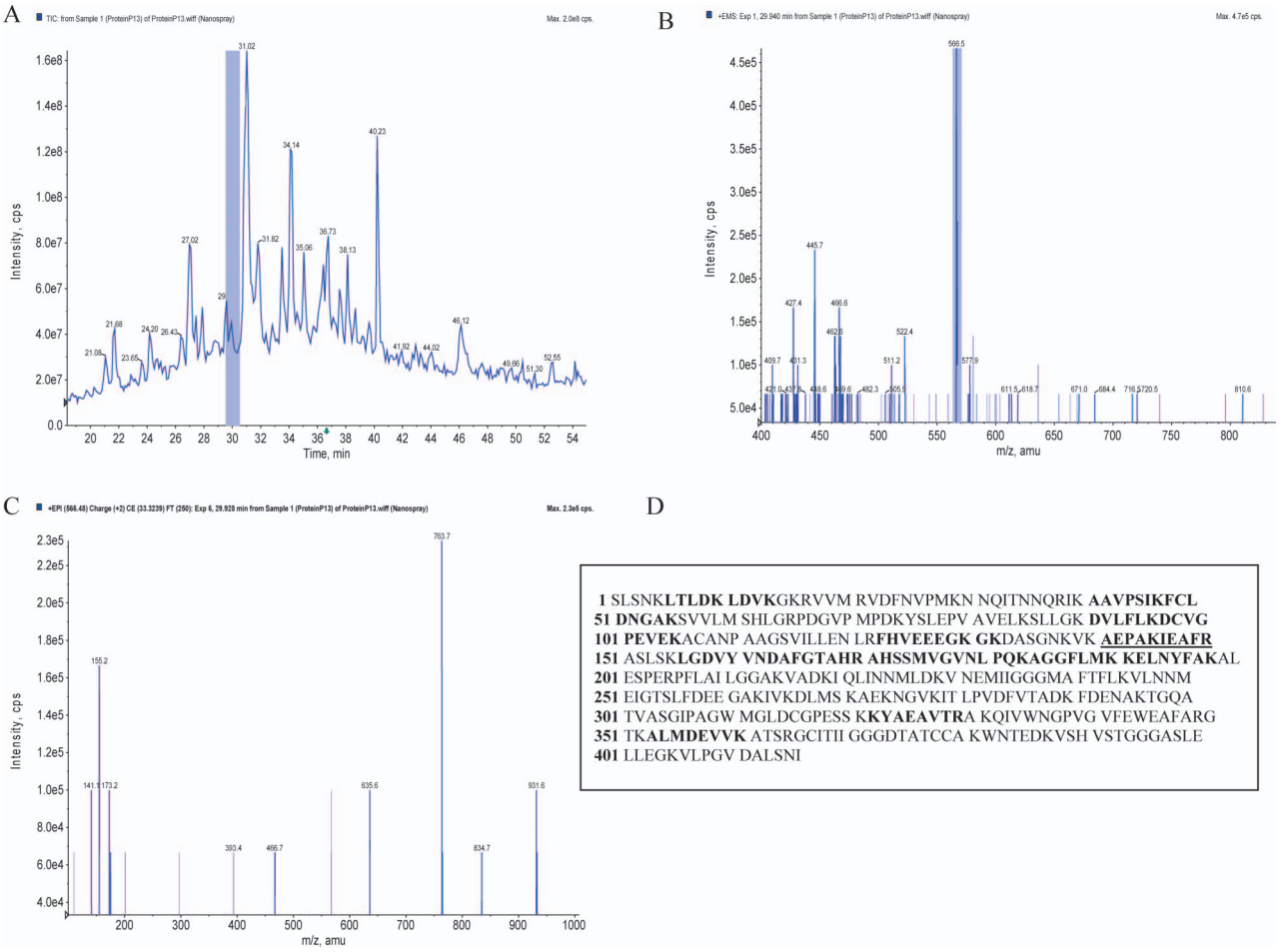

Figure 2. MS analysis of phosphoglycerate kinase-1 (PGK1). Representative results of MS analysis of PGK1, which includes the total ion chromatogram (TIC) of the PGK1 (A), the enhanced MS spectrum (EMS) at the indicated point (t = 30 min) in the chromatogram (B), the MS/MS spectrum (enhanced product ion [EPI]) of the selected peptide in the MS mode (m/z = 565.5) (C) and the entire protein sequence of PGK1 as available in the Swiss-Prot database (D). The peptides identified from the MS/MS spectra of the entire chromatogram (A) are indicated in bold and the underlined peptide is represented in the spectrum C.

of these proteins (ANXA6, ACTB and PGK1) also exhibited modulated phosphorylation levels (Figure 5), we decided to investigate if the corresponding genes underwent changes in expression levels or not. Only three genes that also exhibited alteration in phosphorylation level were found to be significantly down-regulated (ANXA6 and ACTB at 1, 2 and 4 Gy, whereas PGK1 at 2 Gy) following γ-irradiation (Figure 6). TLN2 did not show any significant modulation following γ-irradiation.

Identification of ERG by DNA microarray

The DNA microarray analysis identified 44 ERG, which exhibited at least 2-fold up- or down-regulation of the gene expression (Table III). The Table shows GenBank accession number, gene symbol, biological process, molecular function and relative expression (RE) along with standard deviation of means (SD) and probability of error (P) at 1, 2 and 4 Gy of γ-rays for the identified genes. The RE of the non-irradiated control has been taken as 1.00. All genes, except the docking protein 7 (DOK7), were significantly up-regulated following γ-irradiation.

Validation of gene expression modulation of selected ERG in three donors

Following DNA microarray analysis, several genes have emerged as potential and valuable candidates for radiation biodosimetry. Our previous study on lymphocytes has already reported changes in the expressions of CDKN1A, CD69, EGR1, EGR4, IFN-γ, interferon-stimulated exonuclease gene 20 kDa-like 1 (ISG20L1), c-JUN, MDM2, polo-like kinase 2 (PLK2), rho-family GTPase 1 (RND1) and TNFSF9 genes in six human subjects following 0–4 Gy of γ-irradiation (Turtoi et al. 2008). In the present study we have, therefore, selected another

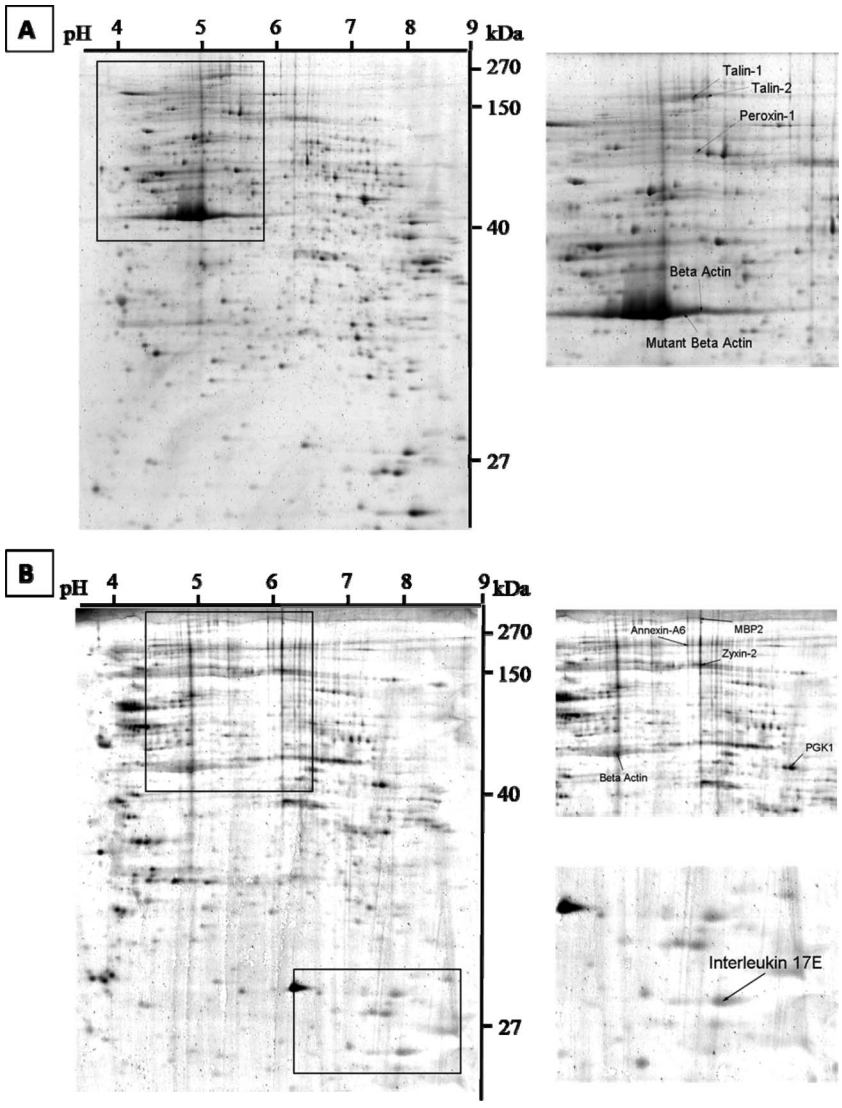

Figure 3. 2D-PAGE protein analysis of irradiated lymphocytes. Sham control lymphocyte proteins separated on 12% SDS-PAGE gels in the pH range of 3–10. Image (A) represents total proteins stained with Sypro-Ruby stain, whereas the image (B) shows the phosphorylated proteins stained with the Pro-Q-Diamond^{TM} dye. The spots indicated by the arrows are proteins identified with the MS that displayed at least two-fold increase or decrease in the concentration as compared with the non-irradiated control at the $P \leq 0.05$ following the γ-irradiation.

group of genes that has not been investigated so far. This group of genes comprised BBC3, DUSP8, GADD45A, PCNA and TRAF4. The modulations of expression of these genes were monitored in three individuals following γ-irradiation of lymphocytes ex-vivo. The results are shown in Figure 7 and Table IV. Significant alterations of gene expression ($RE \geq 2.0$ and $P \leq 0.05$), with at least a trend of dose-dependence, were detected in four of the five genes – BBC3 (individual 3; $R^2 = 0.97$), DUSP8 (individual 3; $R^2 = 0.99$), GADD45A (individuals 1 and 2; $R^2 = 0.97/0.93$) and PCNA (individuals 1 and 3; $R^2 = 0.87/0.94$). However, the trends observed for BBC3 and PCNA in the individual 3 were limited to 0–2 Gy range. For both genes a significant decrease of the relative expression was observed at 4 Gy.

Analysis of cellular proteins employing WB

Following the rationale that there is a significant discrepancy between the gene expression and protein modulation, predominately due to various post-transcriptional events, a validation of several modulated ERG was performed at the protein level. For this purpose, protein products of selected genes showing significant up- or down-regulations following DNA microarray analyses were quantified by WB analysis in three human donors. Four proteins (MDM2, c-JUN, PCNA and CDKN1A) were chosen for this analysis (Figure 8). Two of the proteins, c-JUN and PCNA, did not show significant changes in the protein concentration following γ-irradiation with the exception that PCNA for individuals 2 and 3 and c-JUN for individual 3 displayed significant reduction of respective protein

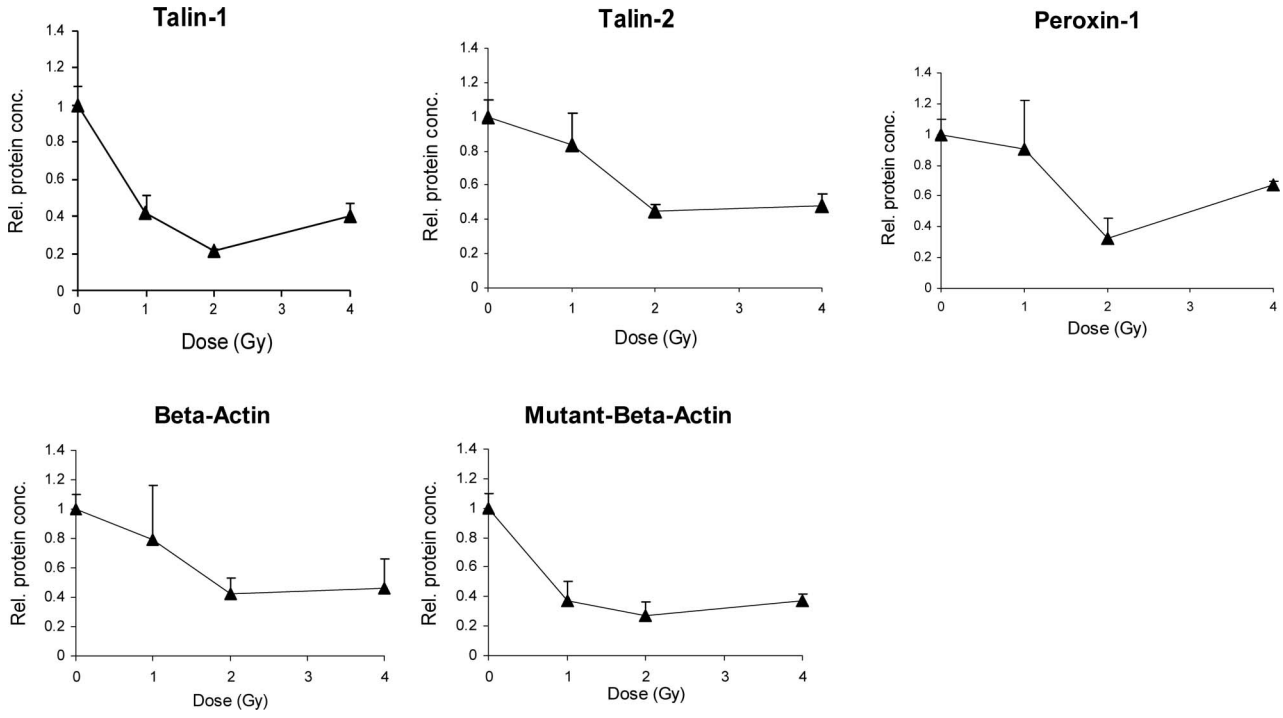

Figure 4. ERPRO response to irradiation. The dose-response plots of five ERPRO that displayed modulated protein concentration in response to γ-irradiation. The data were accrued from the Sypro Ruby^{TM}-stained 12% 2D gels. The standard deviations of the mean (SD) have been plotted only in one direction.

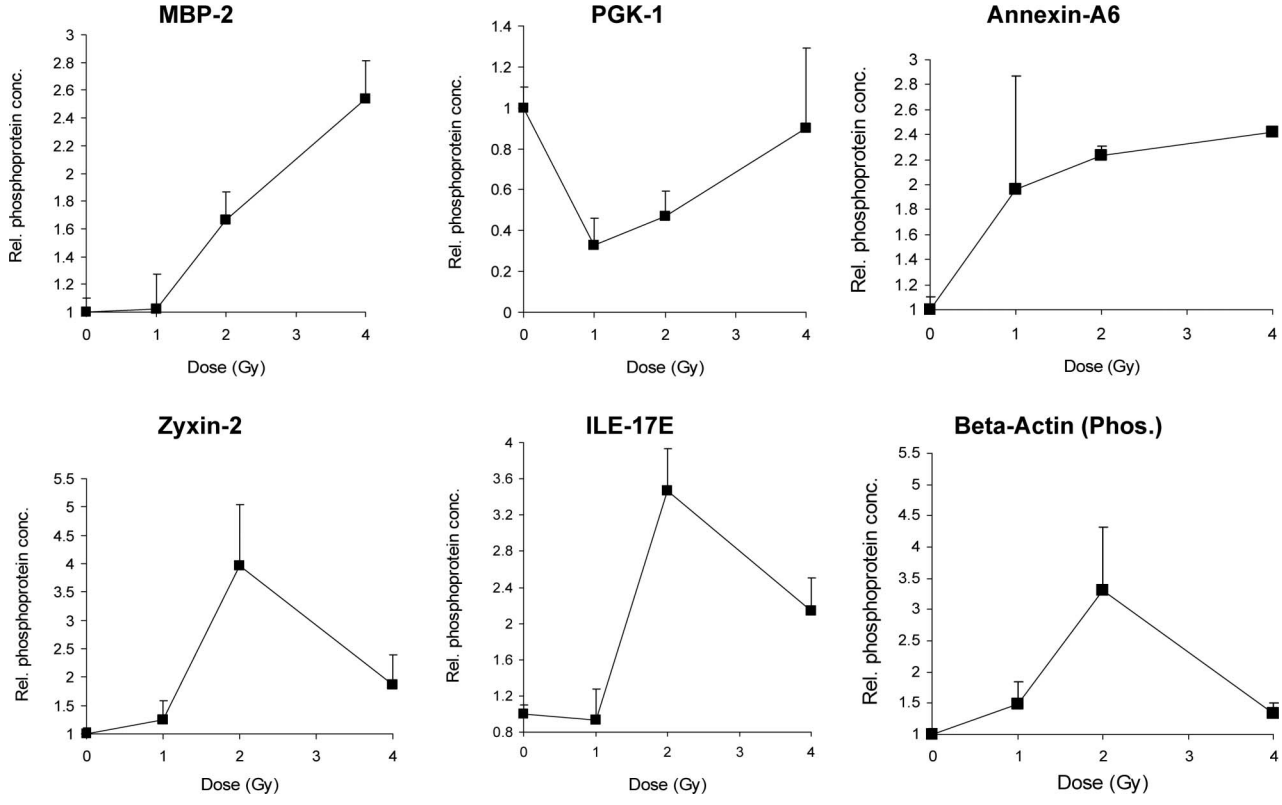

Figure 5. Protein phosphorylation response to irradiation. Human lymphocyte proteins exposed to increasing doses of γ-radiation were subjected to 2D-PAGE on a 12% polyacrylamide gel and stained with Pro-Q Diamond fluorescence stain. Six proteins exhibited modulations in their Pro-Q Diamond stain intensity and pattern; this is potentially indicative for alteration in their state of phosphorylation. The standard deviations of the mean (SD) have been plotted only in one direction ($n = 3$).

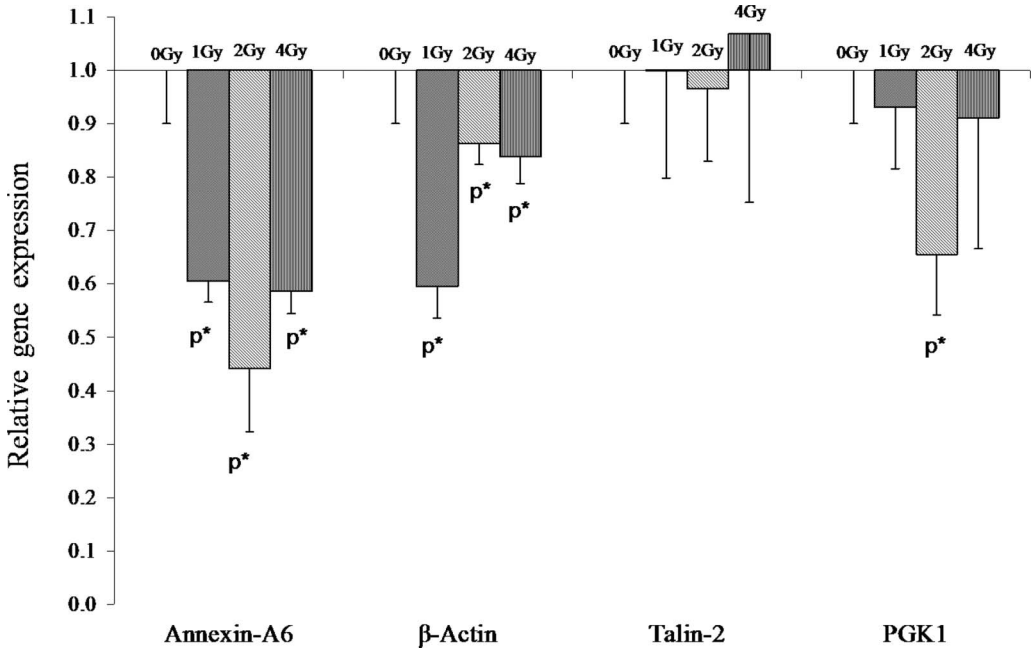

Figure 6. RT-qPCR analysis of ERG. Four selected ERPRO were analysed for possible modulation of their gene expressions using the TaqMan^{TM}-based RT-qPCR. The corresponding TaqMan^{TM} probes are indicated in the Table I. The standard deviations of the mean (SD) have been plotted only in one direction. The p* indicates significance of at least $P = 0.05$ calculated with the two-sided Student's *t*-test ($n = 3$).

concentration at the highest dose. Significant increase in protein concentrations was observed for the other two proteins – MDM2 (individuals 1 and 3 at 1 and 2 Gy) and CDKN1A (individuals 2 and 3 at 1, 2 and 4 Gy).

Discussion

The relatively small number of proteins identified by 2D-PAGE/MS analyses (Figures 2 and 3) as ERPRO exposes the obvious limitation of a solely proteomic approach in identifying biomarkers of exposure to γ-radiation. The limitation appears to be due to: (a) limited dynamic range of the 2D gels (approx. three orders of magnitude) and (b) rather limited sensitivity of MS analysis of the in-gel digested proteins using the proteomic set-up. In order to overcome these limitations and to get a better insight into the proteomic constitution of the cells, DNA microarray and WB techniques have been additionally applied here. It is important to note that the protein alterations in this study are the result of a cumulative effect of ionising radiation on human lymphocytes ex-vivo. Therefore, the observed alterations in the protein concentration could be the result of both the alteration of gene expression and possibly an altered biological half-life of the protein. Ionising radiation generates reactive oxidative species in the cells, which can react with a variety of molecules, including proteins, to potentially build toxic complexes (Stadtman and Levine 2003, Nyström 2005). The accumulation of toxins might influence normal cellular processes.

Although only half of the altered proteins seen on the 2D gels have been identified, the γ-radiation-induced alterations of the structural proteins seem to be very prominent. Significant alterations of TLN1, TLN2, ACTB, mACTB and ZYX2 have been measured (Figure 4). The general trend was a decrease in the concentrations of structural proteins with increasing γ-doses (Figure 4). At the same time, the phosphorylation of ZYX2 and ACTB proteins was found to increase up to 2 Gy (Figure 5). To explain the seemingly contradictory observations, RT-qPCR measurements were performed for ACTB and TLN2. The results showed a minor decrease of the gene expression of ACTB and no alteration of TLN2 (Figure 6). The gene expression pattern of ACTB showed a similar trend compared with the protein alterations. In case of ACTB, the 15- and 31-kDa apoptosis specific protein fragments could not be detected on the gel. These fragments usually arise from the ACTB cleavage and serve as an indicator of apoptotic degradation. These results point out that the decrease of the structural proteins may represent a rather indirect effect of γ-radiation caused by another protein which may not be related to apoptosis.

The genome-wide investigations conducted using the DNA microarrays threw some light on the RND1 gene (see Table III). RND1 is known to phosphorylate several structural proteins, including ACTB,

Table III. The identified ERG in isolated lymphocytes following ex-vivo γ-irradiation of peripheral blood from a human donor. Whole blood collected on three separate days received radiation doses of 1, 2 and 4 Gy. After γ-exposure the lymphocyte fraction was separated (over a period of 2 h at 20°C) and the RNA isolated. The RNA samples were analysed using the DNA microarray technique. Only those genes showing either a significant ($P \leq 0.05$) up- (RE > 2.0) or down-regulation (RE < 2.0) in at least one of the irradiated samples were displayed. Early relative gene expression (RE), SD and the *P*-values (one-way ANOVA) were calculated with respect to non-irradiated control samples which were set to 1.000 ($n = 3$).

				1 Gy			2 Gy			4 Gy		
Genbank	Gene Symbol	Biological Process	Molecular Function	RE	SD	P	RE	SD	P	RE	SD	P
NM_004024	ATF3	*regulation of transcription*	*transcription factor*	**1.724**	0.201	0.001	**2.801**	0.285	0.000	**3.404**	0.352	0.000
BC007549	BAT2D1	*unknown*	*unknown*	**2.470**	1.375	0.024	**3.751**	0.749	0.000	**5.086**	0.627	0.000
NM_014417	BBC3	*apoptosis, caspase activation*	*protein binding*	**3.865**	0.391	0.000	**4.184**	0.709	0.000	**4.617**	0.543	0.000
NM_006763	BTG2	*DNA repair, transcription regulation*	*transcription factor*	**1.404**	0.141	0.002	**1.873**	0.189	0.000	**2.312**	0.233	0.000
NM_001781	CD69	*defense response*	*transmembrane receptor*	**2.851**	0.343	0.000	**3.873**	0.294	0.000	**5.154**	0.444	0.000
NM_001252	CD70	*apoptosis, immune response*	*TNF receptor binding*	**3.272**	0.322	0.000	**3.224**	0.677	0.000	**3.987**	0.441	0.000
NM_004233	CD83	*defense and immune response*	*unknown*	**2.548**	0.254	0.000	**3.573**	0.356	0.000	**4.121**	0.411	0.000
NM_000389	CDKN1A	*cell cycle arrest*	*cyclin-dependent protein kinase*	**2.427**	0.140	0.000	**2.699**	0.425	0.001	**3.014**	0.469	0.000
NM_018947	CYCS	*electron transport, caspase activation*	*cytochrome c oxidase complex*	**1.439**	0.145	0.002	**1.752**	0.176	0.000	**2.547**	0.271	0.000
AK024926	DDAH1	*arginine catabolic process*	*dimethylargininase*	**1.646**	0.168	0.001	**2.016**	0.287	0.000	**2.100**	0.213	0.000
NM_173660	DOK7	*neuromuscular junction development*	*insulin receptor binding*	**0.585**	0.118	0.003	**0.458**	0.051	0.000	**0.440**	0.045	0.000
NM_004418	DUSP2	*inactivation of MAPK activity*	*tyrosine phosphatase*	**1.336**	0.134	0.004	**1.842**	0.335	0.001	**2.619**	0.262	0.000
NM_004419	DUSP5	*protein amino acid dephosphorylation*	*tyrosine phosphatase*	**1.609**	0.159	0.001	**1.715**	0.169	0.000	**2.178**	0.215	0.000
NM_004420	DUSP8	*inactivation of MAPK activity*	*tyrosine phosphatase*	**1.816**	0.185	0.000	**2.558**	0.529	0.000	**3.719**	0.819	0.000
NM_001964	EGR1	*regulation of transcription*	*transcription factor*	**3.339**	0.621	0.000	**7.129**	2.692	0.001	**8.794**	2.395	0.000
NM_153606	FAM71A	*unknown*	*unknown*	**1.318**	0.208	0.055	**2.303**	0.557	0.002	**2.403**	0.276	0.000
NM_001924	GADD45A	*regulation of cyclin dependent PKA*	*protein binding*	**2.778**	0.279	0.000	**2.747**	0.275	0.000	**2.826**	0.526	0.000
NM_005524	HES1	*regulation of transcription*	*transcription regulator*	**6.217**	0.632	0.000	**10.525**	1.705	0.000	**8.508**	0.863	0.000
NM_003538	HIST1H4A	*chromatin organisation*	*DNA binding*	**1.241**	0.137	0.008	**1.965**	0.461	0.002	**2.300**	0.250	0.000
AK097297	HLA-DQB1	*antigen presentation via MHC class II*	*GTP binding, MHC class II receptor*	**1.389**	0.160	0.005	**2.087**	0.216	0.000	**2.304**	0.241	0.000
NM_002127	HLA-G	*antigen presentation via MHC class I*	*MHC class I receptor activity*	**1.285**	0.130	0.007	**1.538**	0.171	0.000	**2.032**	0.204	0.000
NM_021979	HSPA2	*protein folding*	*unfolded protein binding*	**1.645**	0.180	0.001	**2.421**	0.671	0.003	**2.911**	0.716	0.001
NM_016545	IER5	*unknown*	*unknown*	**1.625**	0.164	0.001	**1.953**	0.305	0.000	**2.203**	0.275	0.000
NM_000619	IFNG	*cell-cell signaling, response to virus*	*cytokine activity*	**2.611**	0.646	0.006	**3.038**	1.463	0.024	**6.683**	0.362	0.000
NM_022767	ISG20L1	*apoptosis, response to DNA damage*	*exonuclease activity*	**3.984**	0.639	0.000	**3.314**	0.357	0.000	**3.581**	0.354	0.000
NM_002228	JUN	*regulation of transcription*	*RNA polymerase II transcription factor*	**1.611**	0.071	0.000	**3.367**	0.508	0.000	**3.851**	0.414	0.000
NM_006879	MDM2	*regulation cell cycle progression*	*ubiquitin-protein ligase*	**5.473**	0.545	0.000	**5.791**	0.576	0.000	**5.708**	1.065	0.000
NM_173198	NR4A3	*regulation of transcription*	*transcription factor*	**1.133**	0.113	0.079	**1.707**	0.169	0.000	**2.268**	0.238	0.000
NM_002592	PCNA	*regulation of DNA replication and repair*	*DNA polymerase processivity factor*	**2.961**	0.292	0.000	**2.983**	0.250	0.000	**3.711**	0.546	0.000
NM_015900	PLA1A	*phosphatidylserine metabolism*	*phospholipase A1 activity*	**1.842**	0.220	0.001	**3.015**	1.610	0.019	**3.482**	0.649	0.000
NM_006622	PLK2	*positive regulation of I-KB / NF-KB*		**2.948**	0.292	0.000	**3.572**	0.690	0.000	**4.396**	0.436	0.000
NM_021127	PMAIP1	*induction of apoptosis*	*protein binding*	**2.123**	0.077	0.000	**2.251**	0.127	0.000	**2.911**	0.444	0.000
NM_001198	PRDM1	*negative regulation of transcription*	*transcription factor activity*	**1.329**	0.135	0.004	**1.570**	0.437	0.027	**2.184**	0.222	0.000
NM_002922	RGS1	*immune response, B cell activation*	*GTPase activator, calmodulin binding*	**1.138**	0.114	0.055	**2.318**	0.566	0.002	**2.780**	0.335	0.000
NM_014470	RND1	*actin filament organization*	*GTPase activity*	**2.483**	0.269	0.000	**2.355**	1.324	0.055	**3.794**	0.775	0.000
NM_080860	RSPH1	*meiosis*	*unknown*	**1.974**	0.246	0.000	**2.668**	0.359	0.000	**3.721**	0.758	0.000
NM_138356	SHF	*apoptosis*	*protein binding*	**1.640**	0.259	0.000	**1.810**	0.430	0.004	**2.478**	0.271	0.000

(*continued*)

Table III. (*Continued*)

Genbank	Gene Symbol	Biological Process	Molecular Function	1 Gy			2 Gy			4 Gy		
				RE	SD	P	RE	SD	P	RE	SD	P
NM_138810	TAGAP	*signal transduction*	*guanyl-nucleotide exchange factor*	**1.887**	0.187	0.000	**2.042**	0.202	0.000	**2.256**	0.223	0.000
NM_031272	TEX14	*protein amino acid phosphorylation*	*protein kinase*	**1.300**	0.215	0.020	**1.697**	0.252	0.000	**2.134**	0.223	0.000
NM_003811	TNFSF9	*apoptosis, immune response*	*TNF receptor binding*	**2.644**	0.257	0.000	**2.834**	0.272	0.000	**3.028**	0.291	0.000
NM_004295	TRAF4	*apoptosis, protein ubiquitination*	*DNA binding, ubiquitin-protein ligase*	**2.514**	0.254	0.000	**3.095**	0.312	0.000	**3.688**	0.372	0.000
AK097045	WDR79	*unknown*	*unknown*	**1.540**	0.221	0.004	**1.794**	0.209	0.001	**2.579**	0.293	0.000
NM_023929	ZBTB10	*regulation of transcription*	*DNA and protein binding*	**1.701**	0.180	0.000	**1.968**	0.203	0.000	**2.532**	0.261	0.000

and is responsible for their depolymerisation and reorganisation. Its gene expression is controlled by c-JUN that was up-regulated in DNA microarray studies (see Table III). Protein measurements conducted with WB could not confirm these results in three individual donors tested (Figure 7). This discrepancy cannot be fully explained from the data available and warrants further study. It is possible that a rapid degradation of this transcription factor or a time delay between gene expression and protein synthesis may have contributed to the observation. However, the available data clearly indicates that ionising radiation activates the transcription factor AP-1 whose major part is c-JUN, which, in turn, activated the expression of the RND1 gene. Most probably, the RND1 protein leads to the depolymerisation and rearrangements of structural proteins, including ACTB and ZYX1. Chen et al. (2005) have shown radiation-induced modulation of ACTB in the bone marrow macrophages. They compared two different populations of macrophages originating from two mouse strains (C57Bl/6 and CBA/Ca) 24 h after in vivo γ-irradiation (0.5 Gy). After irradiation, an increase of ACTB concentration by a factor of 3.1 was observed. Interestingly, the corresponding ACTB spot on the 2D gel revealed that the molecular weight was 30 kDa. No clear explanation was given as to what might have influenced this molecular weight reduction. Considering the results presented in this report, apoptotic degradation or structural reorganisation may be one of the possible reasons. Zhang et al. (2005) have reported in IEC-6 rat epithelial cells a significant reduction of vimentin and β-tubulin protein concentrations 24 h after γ-irradiation (25 Gy). These studies highlight possible important role(s) of structural proteins in cellular radiation response. They also point at the need of further investigation to understand these processes.

Another group of genes and proteins that appears to be affected at an early stage after exposure to ionising radiation are those involved in cell cycle controls (Figures 5, 8 and Table III). The result of this investigation further differentiates them into two subgroups. The first one comprises proteins and genes which participate in the RAS/RAF signalling pathway and, in turn, activate mitogen-activated protein kinase (MAPK) to induce cell cycle progression. ANXA6 is one such protein. It is a calcium-dependent protein that induces the RAS-p120GAP complex formation. Its phosphorylation was found to increase with increasing γ-dose (Figure 5). However, the results of the gene expression study did not provide further clarity as to the reason of the observed change of the phosphorylation state. The RT-qPCR investigation pointed at a potential decrease of the ANXA6 gene expression (Figure 6).

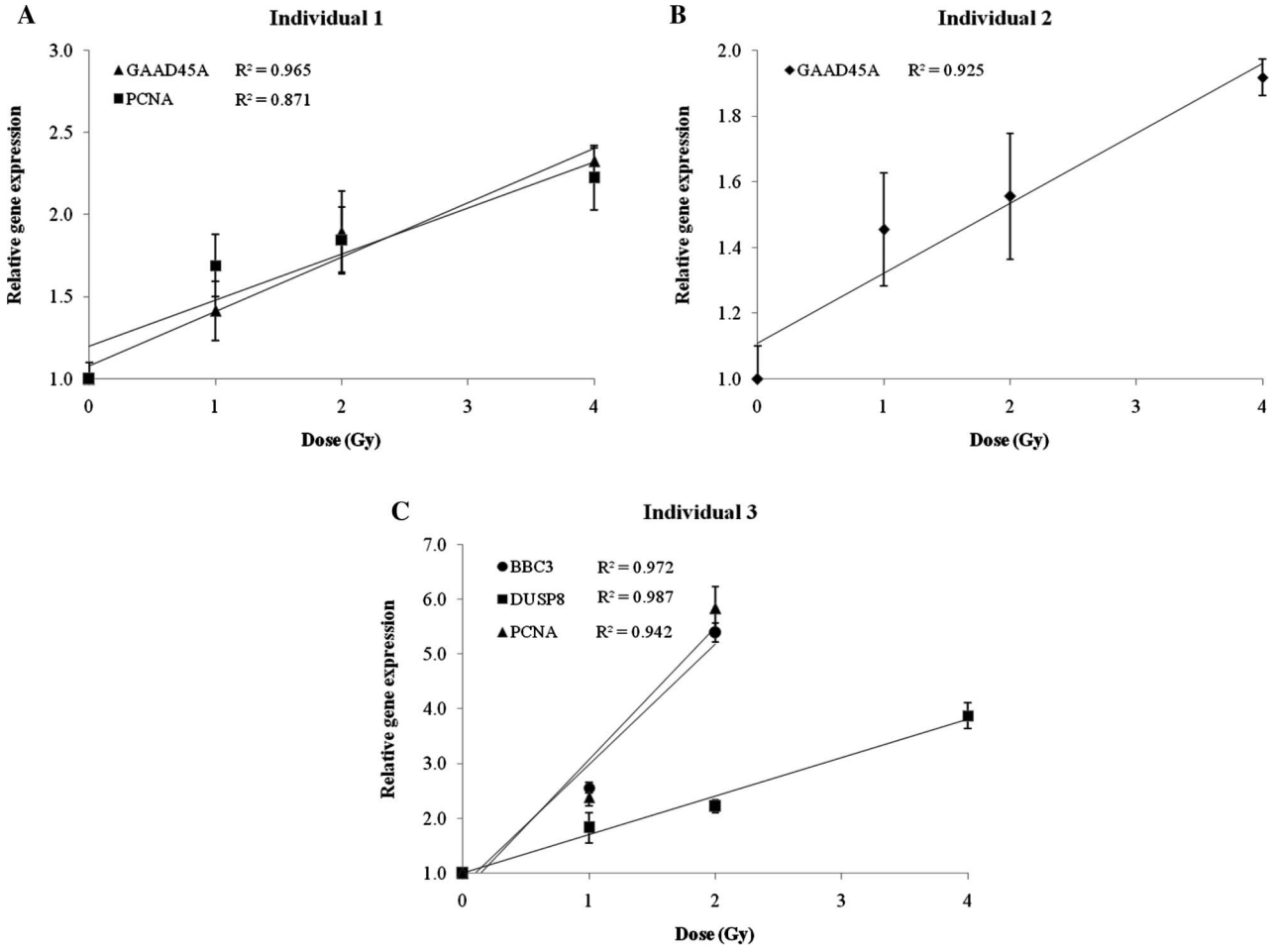

Figure 7. (A–C) Validation of ERG response in individual donors. The relative expression of up-regulated ERG identified in γ-irradiated lymphocytes from human peripheral blood of three individuals as measured by the RT-qPCR. Only genes showing linear trends were considered. The dose dependence over the range 1–4 Gy was assessed by linear regression analysis. RE of the genes BBC3 and PCNA in the individual 3 were only measured up to 2 Gy. Standard deviations of data points for each individual were taken from Table IV.

Table IV. The relative expression (RE) of selected ERG in lymphocytes following ^{137}Cs γ-irradiation (1–4 Gy) was determined in three individuals using the TaqMan^{TM} RT-qPCR. The RE and SD (standard deviation of means) were calculated with respect to non-irradiated control samples which were set to 1.000.

		Individual no.					
		1		2		3	
Gene	Dose (Gy)	RE	SD	RE	SD	RE	SD
BBC3	1	1.26	0.08	0.73	0.07	2.56	0.10
	2	1.18	0.15	0.64	0.08	5.40	0.17
	4	1.20	0.01	0.39	0.05	4.01	0.07
DUSP8	1	1.57	0.08	1.01	0.14	1.83	0.28
	2	1.40	0.11	0.83	0.01	2.22	0.12
	4	2.08	0.05	1.30	0.08	3.88	0.24
GAAD45A	1	1.42	0.18	1.46	0.17	0.52	0.02
	2	1.89	0.25	1.56	0.19	0.64	0.05
	4	2.33	0.08	1.92	0.05	0.82	0.01
PCNA	1	1.69	0.19	1.24	0.10	2.39	0.16
	2	1.85	0.20	1.37	0.07	5.84	0.40
	4	2.23	0.20	1.09	0.03	4.35	0.48
TRAF4	1	1.69	0.14	0.63	0.01	1.05	0.01
	2	1.56	0.24	0.72	0.02	8.64	0.85
	4	1.93	0.21	0.71	0.03	3.39	0.30

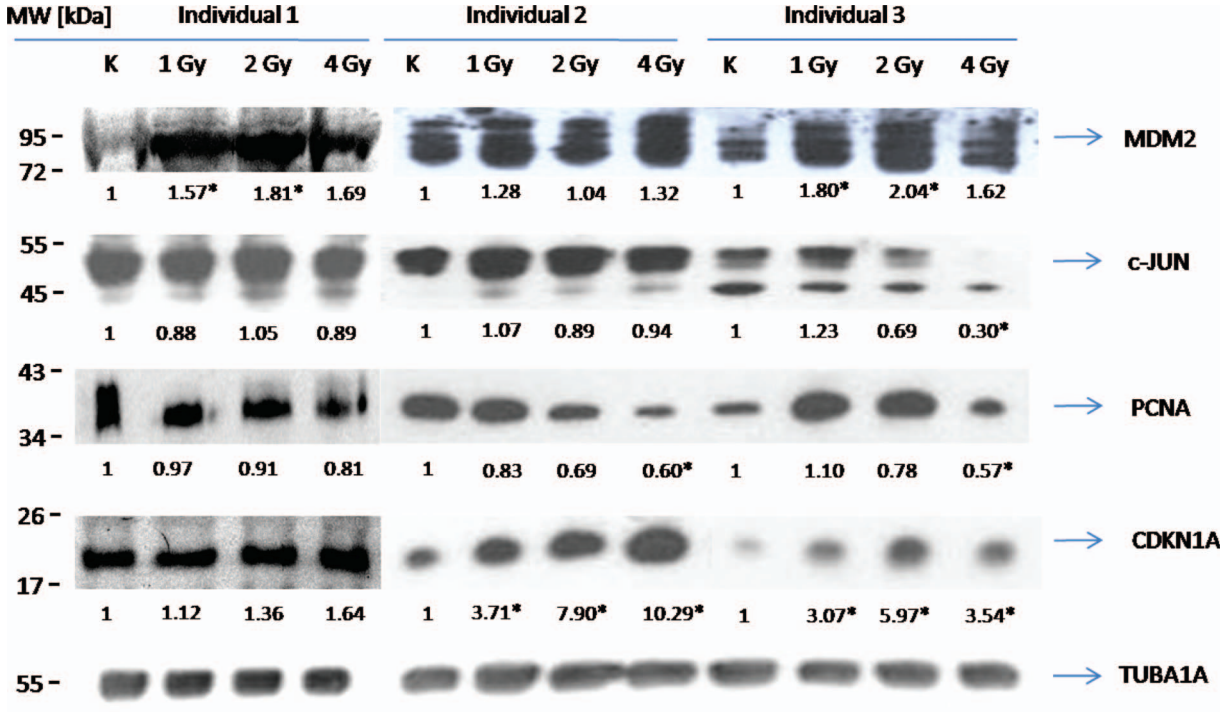

Figure 8. WB analysis of selected ERPRO. WB analysis of four selected proteins (MDM2, c-JUN, PCNA and CDKN1A) and their dose-dependant alterations of protein concentration with respect to non-irradiated controls (set as 1.00). The normalisation was conducted with respect to the TUBA1A values. The numbers indicate average values whereas * indicates significant result at the $P \leq 0.05$ level.

This contradiction cannot be explained with the data obtained in the present study. However, assuming that ANXA6 is activated through phosphorylation, it would induce the RAS-p120GAP complex formation and, in turn, inactivate RAS, which may halt the cell cycle progression (King and Sartorelli 1986). DNA microarray analysis support the assumption as it shows up-regulation of dual specificity phosphatase-2, 5 and 8 (DUSP2, DUSP5 and DUSP8) genes, which code for phosphatases that dephosphorylate their target kinases (see Table III). These genes negatively regulate MAPK superfamily proteins, which are associated with cellular proliferation. Several proteins and genes that are directly involved in the cell cycle control were also found to be altered after the exposure to γ-radiations. One of the most prominent candidates belonging to this group is MDM2 protein whose modulated concentration and gene expression patterns were detected (see Table III and Figure 8). In this study, increased gene expression as well as protein concentration of CDKN1A were measured (see Table III and Figure 8). Bae et al. (1995) have shown p53 regulation of CDKN1A after γ-irradiation, which caused p53 mediated G_1-arrest in Burkitt's lymphoma wild-type cells. The authors demonstrated that both protein concentration and gene expression of CDKN1A changed rapidly after irradiation reaching the highest level within 4 h. In addition, either as a direct consequence of alteration in the RAS/RAF or p53 signalling pathways, another cell cycle regulatory gene, GADD45A, was up-regulated. GADD45A is a gene whose expression is reported to increase following treatment with DNA damaging agents, including ionising radiation (Smith et al. 2000). The measurements of gene expression and protein concentration do not reveal a large number of genes that are directly involved in DNA repair except PCNA. Our results show up-regulation of PCNA gene expression (Table III) without a significant alteration in its protein concentration (Figure 8).

From the observations made in this section of the investigation, it can be postulated that γ-radiation induces immune system-mediated responses in lymphocytes. Both DNA microarray and 2D-PAGE analyses showed a series of altered genes and proteins that are involved in immunity and defence reactions (Figure 9). Two of the first identified γ-radiation modulated proteins belonging to this group are MBP2 and IL17E. Both proteins were found to be increasingly phosphorylated in response to increasing γ-doses. The dose-response trend appeared to exist for MBP2 between 1 and 4 Gy, whereas IL17E showed a rapid increase between 0 and 2 Gy followed by a significant decrease at 4 Gy (Figure 5). MBP2 interacts with the DNA enhancer elements of genes coding for MHC-I, interleukin-2 and interferon proteins (Van't Veer et al. 1992). These proteins are mainly responsible for cellular defence processes. The subsequent DNA microarray

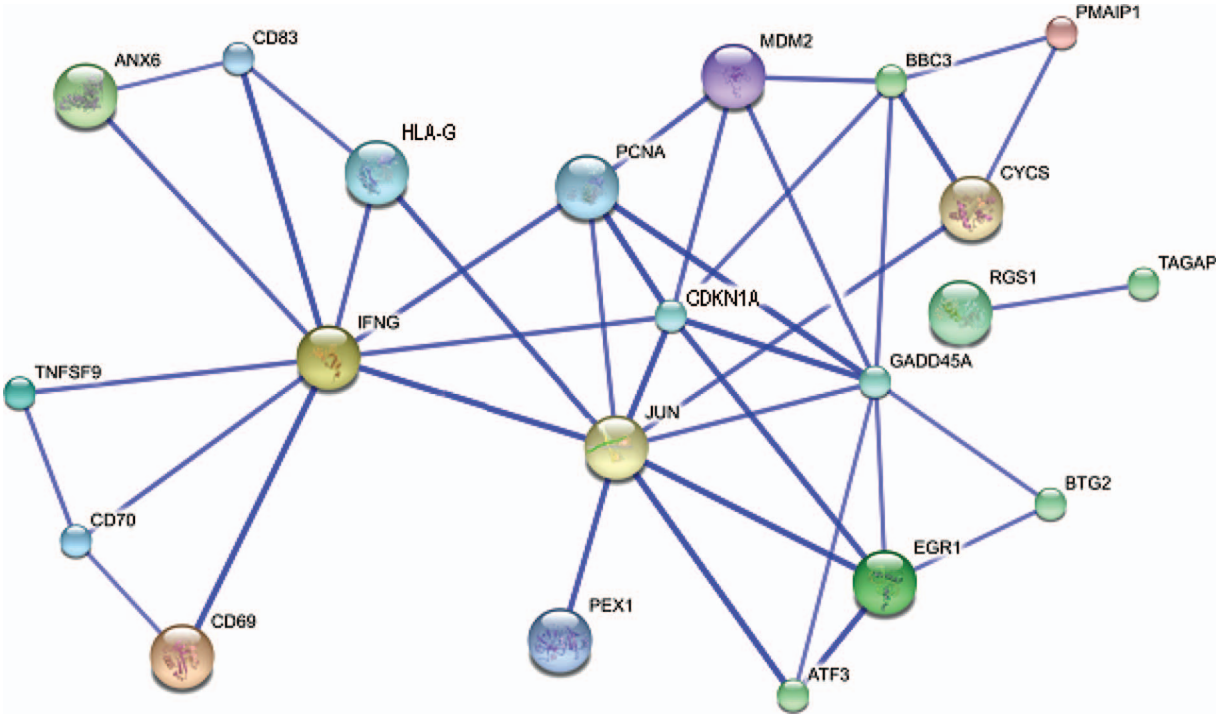

Figure 9. Schematic network of major genes and proteins. This functional hypothetical network depicts the possible correlation between selected proteins and genes, which showed significant modulation following γ-irradiation of human lymphocytes (Figures 3–6 and Table III). The analysis was based on the software, STRING 8.0 (Jensen et al. 2008).

analysis could confirm the up-regulation of the IFNG gene. IL17E is involved in the activation of the nuclear factor of kappa light polypeptide enhancer in B cells (NF$\kappa\beta$), and it enhances the production of interleukin-8. Both proteins are related to apoptosis and immune processes.

Protein degradation is a down-stream biological process that is involved in the acute response of the lymphocytes to γ-radiation. This study measured a decreased concentration of PEX1 protein in response to γ-irradiation (see Figure 4). PEX1 plays a role in protein transport to the peroxisomes, thereby, facilitating their degradation. However, its diminished level in response to the γ-irradiation cannot be easily explained. Among many possible biological reasons, PEST sequence may be one. PEX1 shows a PEST sequence near the C-terminus (see Table II). According to Rechsteiner and Rogers (1996), the C-terminal PEST sequences are particularly relevant for the ubiquitine-dependent protein degradation. On the other hand, some recent findings suggest that PEST regions may not exhibit any preference to be localised in the C-terminal regions and that these motifs may be found in nearly 25% of the entire proteome (Singh et al. 2006). Therefore, the discussion remains inconclusive at this stage and more work is needed to explain it. Recently, Turtoi et al. (2008) have reported down-regulation of serine hydrolase-like gene 2 (SERHL2) following γ-irradiation of human lymphocytes. SERHL2 is found in peroxisomes taking part in protein hydrolysis and degradation. Apart from the similarities in the expression/concentration patterns, both SERHL2 and PEX1 indicate a possible role of peroxisomes in the acute cellular response following γ-irradiation.

Finally, the modulated PGK1 concentration in response to γ-irradiation points to the importance of glycolysis in radiation response of lymphocytes. The 2D-PAGE revealed a general reduction of the phosphorylation of PGK1 in respect to the non-irradiated controls. This was evident at 1 Gy, where the decrease was at a maximum. From 2 Gy onwards, the trend reversed (Figure 5). The phosphorylation of PGK1 recovered completely at 4 Gy. The radiation response of PGK1 cannot be explained completely based on the results of this investigation. Nonetheless, it is known from the work of Chandel et al. (1998) that ROS can directly mimic the ionising radiation-inducing expression of PGK1 gene. Our results show the change of PGK1 phosphorylation status (Figure 5) and a down-regulation of its gene expression (Figure 6) after exposure of lymphocytes to γ-radiation. PGK1 is a key enzyme of glycolysis and, hence, its deregulation can lead to short supply of energy in cells. Several investigators have shown changes in the concentration of various glycolysis enzymes following exposure of mammalian cells to γ-irradiation. Zhang et al. (2003) have shown using 2D-PAGE an increase of PGK2 concentration in

epithelial cells of intestine 3 h after their exposure to ionising radiations (9 Gy). Lu et al. (2006) found a decrease in the concentration of enolase in glioblastoma cells 24 h after exposure to ionising radiation (7 Gy).

In conclusion, a satisfactory explanation for radiation-induced alterations of protein concentration and gene expression remains elusive. It is to be noted that it does not take into account the mechanisms of post-transcriptional gene expression regulation (e.g., miRNA measurements). Nevertheless, the alteration of the protein concentrations can be viewed as an immediate cellular response whereas the changes of the gene expression might give clues as to what action the cells might take in the near future. The results of this investigation focus on the acute proteome alterations after exposure to γ-radiation in clinical and mild to moderate dose range. The data acquired could offer a basis for consideration of biomarkers as radiation dose indicators. It is to be noted that the data presented here are for a 2 h post-irradiation period only. Although it would be desirable to see the effects at 12- and 24-h post-irradiation periods, we have not succeeded in performing such experiments due to a significant degradation of mRNA and enhanced level of apoptosis at 6-, 12- and 24-h following γ-irradiation (unpublished results). Expanding the observation period for several hours could provide additional important data. Nevertheless, caution is required while dealing with lymphocytes as the majority of them rapidly enter apoptosis, which was measured in at least 20% of the γ-irradiated cells 6 h after 2 Gy ^{137}Cs γ-ray irradiation (unpublished results). Degradation of RNA is an issue which may also prevent confident gene expression analysis (Debey et al. 2004). After radiation exposure in vivo, lymphocytes readily leave the blood circulation to invade the surrounding tissue. This brings about the question of appropriate sampling time for an eventual biodosimetric purpose. The inherent fragile nature of mRNA may limit the applicability of ERG or ERPRO markers of lymphocytes for biodosimetry to a post-irradiation period of only a few hours. Another limitation of this approach could be the problem of individual variability. The results presented in this report represent the individual status of three human donors on the three different sampling days (Figure 7). The data cannot be seen as representative since factors like illness and other life-style factors of the individuals may significantly influence the basal levels of gene expression and protein concentration. Nonetheless, this study does narrow the cellular response to γ-radiation to the most significant ERG and ERPRO and, hence, offers a possibility to focus further investigations on a selected group of proteins and genes.

Summary and outlook

The investigations of gene expression and proteomic reactions with the help of 2D-PAGE, DNA microarray as well as WB and RT-qPCR have proved to be a promising approach in study of radiation-induced cellular alterations. The all-encompassing approach has revealed early alterations of the protein concentrations of talin-1, talin-2, β-actin, mutant β-actin, peroxin-1, mouse double minute-2, cyclin-dependent kinase inhibitor 1 as well as the phosphorylation status of annexin-A6, MHC-binding protein-2, zyxin-2, interleukin-17E and phosphoglycerate kinase-1. Among them, talin-1 and annexin-A6 (in the dose range 0–2 Gy) and MHC-binding protein-2 (1–4 Gy) displayed near-linear like dose-response trends and, hence, appear to be suitable candidates for biodosimetric applications. Gene expression studies have identified 43 genes that displayed significant changes in their expression following γ-irradiation. Of these BBC3, DUSP8, GADD45A and PCNA seem to be of value as potential biodosimetric markers of acute exposure to clinical levels of ionising radiation (see Figure 9). Their individual dose responses were essentially linear for certain individuals and dose ranges. The majority of the lymphocyte ERPRO and ERG suggest early radiation-induced cellular changes of the cytoskeleton, proliferation and cell cycle, immunoreactions as well as protein degradation and glycolysis. The results warrant further studies involving more individuals and post-irradiation sampling times to fully exploit their applied biodosimetric potentials.

Acknowledgements

This work was supported by a grant from the German Federal Ministry of Education and Research. The authors AT and FHS are former employees of the Research Centre Juelich (FZJ) and are particularly grateful to JuLumni-Net (FZJ) as well as to Dr Reinhard Lennartz (Director of the Department of Safety and Radiation Protection, FZJ) for enabling the completion of this study.

Declaration of interest: The authors report no conflicts of interest. The authors alone are responsible for the content and writing of the paper.

References

Amundson SA, Do KT, Shahab S, Bittner M, Meltzer P, Trent J, Fornace AJ. 2000. Identification of potential mRNA biomarkers in peripheral blood lymphocytes for human exposure to IR. Radiation Research 154:342–346.

Amundson SA, Grace MB, Mcleland CB, Epperly MW, Yeager A, Zhan Q, Greenberger JS, Fornace AJ. 2004. Human *in vivo*

radiation-induced biomarkers: Gene expression changes in radiotherapy patients. Cancer Research 64:6368–6371.

Bae I, Fan S, Bhatia K, Kohn KW, Fornace AJ, O'Connor PM. 1995. Relationship between G1 arrest and stability of the p53 and $P21^{Cip1/Waf1}$ proteins following γ-irradiation of human lymphoma cells. Cancer Research 55:2387–2393.

Chandel NS, Maltepe E, Goldwasser E, Mathieu CE, Simon MC, Schumacker PT. 1998. Mitochondrial reactive oxygen species trigger hypoxia-induced transcription. Proceedings of the National Academy of Sciences of the USA 29;95(20):11715–11720.

Chen C, Boylan MT, Evans CA, Whetton AD, Wright EG. 2005. Application of two-dimensional difference gel electrophoresis to studying bone marrow macrophages and their in vivo responses to ionizing radiation. Journal of Proteome Research 4:1371–1380.

Debey S, Schoenbeck U, Hellmich M, Gathof BS, Pillai R, Zander T, Schultze JL. 2004. Comparison of different isolation techniques prior gene expression profiling of blood derived cells: Impact on physiological responses, on overall expression and the role of different cell types. The Pharmacogenomics Journal 4:193–207.

Dressman HK, Muramoto GG, Chao NJ, Meadows S, Marshall D, Ginsburg GS, Nevins JR, Chute JP. 2007. Gene expression signatures that predict radiation exposure in mice and humans. PLOS Medicine 4:1–12.

Fotedar R, Bendjennat M, Fotedar A. 2004. Role of p21WAF1 in the cellular response to UV. Cell Cycle 3(2):134–137.

Jensen LJ, Kuhn M, Stark M, Chaffron S, Creevey C, Muller J, Doerks T, Julien P, Roth A, Simonovic M, Bork P, von Mering C. 2009. STRING 8–a global view on proteins and their functional interactions in 630 organisms. Nucleic Acids Res. 37(Database issue):D412-6. Epub 2008 Oct 21.

Kang CM, Park KP, Song JE, Jeoung DI, Cho CK, Kim TH, Sangwoo B, Lee SJ, Lee YS. 2003. Possible biomarkers for IR exposure in human peripheral blood lymphocytes. Radiation Research 159:312–319.

King ICL, Sartorelli AC. 1986. The relationship between epidermal growth factor receptors and the terminal differentiation of A431 carcinoma cells. Biochemical and Biophysical Research Communications 140(3):837–843.

Lu X, de la Pena L, Barker C, Camphausen K, Tofilon PJ. 2006. Radiation-induced changes in gene expression involve recruitment of existing messenger RNAs to and away from polysomes. Cancer Research 66:1052–1061.

Marchetti F, Coleman MA, Jones IM, Wyrobek AJ. 2006. Candidate protein biodosimeters of human exposure to IR. International Journal of Radiation Biology 82:605–639.

Nyström T. 2005. Role of oxidative carbonylation in protein quality control and senescence. The European Molecular Biology Organization Journal 24:1311–1317.

Ossetrova NI, Farese AM, MacVittie TJ, Manglapus GL, Blakely WF. 2007. The use of discriminant analysis for evaluation of early-response multiple biomarkers of radiation exposure using non-human primate 6-Gy whole-body radiation model. Radiation Measurements 42(6–7):1158–1163.

Rechsteiner M, Rogers SW. 1996. PEST sequences and regulation by proteolysis. Trends Biochem Sci. 21(7):267–271.

Singh GP, Ganapathi M, Sandhu KS, Dash D. 2006. Intrinsic unstructuredness and abundance of PEST motifs in eukaryotic proteomes. Proteins 62(2):309–315.

Smith ML, Ford JM, Hollander MC, Bortnick RA, Amundson SA, Seo YR, Deng CX, Hanawalt PC, Fornace AJ Jr. 2000. p53-mediated DNA repair responses to UV radiation: Studies of mouse cells lacking p53, p21, and/or gadd45 genes. Molecular Cell Biology 20(10):3705–3714.

Stadtman ER, Levine RL. 2003. Free radical-mediated oxidation of free amino acids and amino acid residues in proteins. Amino Acids 25(3–4):207–218.

Szkanderova S, Port M, Stulik J, Hernychova L, Kasalova I, Van Beuningen D, Abend M. 2003. Comparison of the abundance of 10 radiation-induced proteins with their differential gene expression in L929 cells. International Journal of Radiation Biology 79(8):623–633.

Szkanderova S, Vavrova J, Hernychova L, Neubauerova V, Lenco J, Stulik J. 2005. Proteome alterations in gamma-irradiated human T-lymphocyte leukemia cells. Radiation Research 163:307–315.

Turtoi A, Srivastava A, Sharan RN, Oskamp D, Hille R, Schneeweiss FHA. 2007. Early response of lymphocyte proteins after γ-radiation. Journal of Radioanalytical and Nuclear Chemistry 274:435–439.

Turtoi A, Brown I, Oskamp D, Schneeweiss FHA. 2008. Early gene expression in human lymphocytes after γ-radiation – a genetic pattern with potential for biodosimetry. International Journal of Radiation Biology 84(5):375–387.

Van't Veer LJ, Lutz PM, Isselbacher KJ, Bernards R. 1992. Structure and expression of major histocompatibility complex-binding protein 2, a 275 kDa zinc finger protein that binds to an enhancer of major histocompatibility complex class I genes. Proceedings of the National Academy of Sciences of the USA 89:8971–8975.

Whiteley W, Jackson C, Lewis S, Lowe G, Rumley A, Sandercock P, Wardlaw J, Dennis M, Sudlow C. 2009. Inflammatory markers and poor outcome after stroke: A prospective cohort study and systematic review of interleukin-6. PLoS Medicine 6(9).

Zhang B, Su YP, Ai GP, Liu XH, Wang FC, Cheng TM. 2003. Differentially expressed proteins of gamma-ray irradiated mouse intestinal epithelial cells by two-dimensional electrophoresis and MALDI-TOF mass spectrometry. World Journal of Gastroenterology 9:2726–2731.

Zhang B, Yongping S, Fengchao W, Guoping A, Yongjiang W. 2005. Identification of differentially expressed proteins of gamma-ray irradiated rat intestinal epithelial IEC-6 cells by two-dimensional gel electrophoresis and matrix-assisted laser desorption/ionization-time of flight mass spectrometry. Proteomics 5:426–432.